Article

Enhanced ANN Predictive Model for Composite Pipes Subjected to Low-Velocity Impact Loads

Emad Ghandourah [1], Samir Khatir [2,*], Essam Mohammed Banoqitah [1],
Abdulsalam Mohammed Alhawsawi [1], Brahim Benaissa [3] and Magd Abdel Wahab [2]

1   Nuclear Engineering Department, Faculty of Engineering, King Abdulaziz University,
    Jeddah 21589, Saudi Arabia
2   Soete Laboratory, Department of Electrical Energy, Metals, Mechanical Constructions and Systems,
    Faculty of Engineering and Architecture, Ghent University, 9052 Ghent, Belgium
3   Design Engineering Laboratory, Toyota Technological Institute, Nagoya 468-8511, Japan
*   Correspondence: khatir_samir@hotmail.fr

Abstract: This paper presents an enhanced artificial neural network (ANN) to predict the displacement in composite pipes impacted by a drop weight having different velocities. The impact response of fiber-reinforced polymer composite pipes depends on several factors including thickness, stacking sequence, and the number of layers. These factors were investigated in an earlier study using sensitivity analysis, and it was found that they had the most prominent effect on the impact resistance of the composite pipes. In this present study, composite pipes with a diameter of 54 mm are considered to explore the damages induced by low-velocity impact and the influence of these damages on their strength. To evaluate the effect of low-velocity, the pipes were exposed to impacts at different velocities of 1.5, 2, 2.5, and 3 m/s, and preliminary damage was initiated. Next, we used Jaya and E-Jaya algorithms to enhance the ANN algorithm for good training and prediction. The Jaya algorithm has a basic structure and needs only two requirements, namely, population size and terminal condition. Recently, Jaya algorithm has been widely utilized to solve various problems. Due to its single learning technique and limited population information, Jaya algorithm may quickly be trapped in local optima while addressing complicated optimization problems. For better prediction, an enhanced Jaya (E-Jaya) algorithm has been presented to enhance global searchability. In this study, ANN is enhanced based on the influential parameters using E-Jaya to test its effectiveness. The results showed the effectiveness of the E-Jaya algorithm for best training and prediction compared with the original algorithm.

Keywords: composite pipes; impact loads; ANN; Jaya; E-Jaya

1. Introduction

Fiber-reinforced polymers are used in a wide range of applications in civil and mechanical engineering structures. Because of their high strength-to-weight and stiffness-to-weight ratios, these structures are intended to sustain stresses that ordinary metals cannot handle without sacrificing weight. Most of these structures are intended to withstand tensile and internal pressure loads, but they also face impact loads over their operating lifetimes. Metals impact behavior is well understood and can be precisely predicted. However, the behavior of fiber-reinforced composites is highly complex when it comes to impact stresses, which can cause internal damage and stiffness loss, yet the damage is typically undetectable during visual inspection [1]. Delamination, fiber breakage, and matrix cracking are frequently caused by impact loads [2]. Because of the unusual layered architecture and the presence of heterogeneous components, fiber-reinforced polymeric composites have different damage mechanics from ordinary metals. A variety of experimental studies have been conducted to investigate the behavior of composite plates [3,4], as well as numerical studies [5–9], and analytical studies [10–14]. Impact-sensitive GRP pipes generate

localized interior damage that cannot be detected by visual inspection after the impact. Matrix cracks in the fiber orientation, delamination, and transfer splitting effects between layers, significant debonding, and fiber breaking damages occur in composite pipes after impact. GRP pipes lose strength because of these defects, which increase under static or alternate loads. Furthermore, these damages result in internal pressure leakage. As a result, low-velocity impact behaviors and impact modes of composite structures must be determined. Various studies on low-velocity impact reactions and damage assessments of composite pipes have been published in the literature. Damage development was analyzed in Ref. [15], considering filament wound thin-walled GRP pipes built of S-glass and E-glass under drop weight impact behaviors. In composite plates subjected to low-velocity impact, several failure modes, such as fiber rupture, delamination, mechanical damage, plastic deformations, and significant displacements, have been reported in Ref. [6]. Layer-Wise Theory (LWT) was used by Rafiee et al. [16] to assess in-the-plane and out-of-plane impact-generated failure modes in composite pipes. Moreover, the authors found that the LWT was more effective than the finite element method (FEM) and higher-order shear deformation theory (HOSDT). The mechanical and impact characteristics of fiber-reinforced composite pipes have been studied by several researchers [17,18]. In Ref. [19], the authors studied the burst strength of GRP pipes that were exposed to nonpenetrating impact. Next, Ref. [20] examined the impact behaviors of composite tubes when fatigue loading was applied. The effects of filament wound pipe impact resistance on pipe burst pressures were examined in Ref. [21]. The obtained results found that impact damage reduced the bursting pressure of glass/epoxy tubes substantially. Finite element analysis of composite plates was used to extract the data using ANN to predict the absorbed energy based on low-velocity impact loads [22]. Maziz et al. [23] presented numerical and experimental analyses of composite pipes under the low-velocity impact and a progressive damage model for pressurized filament wound.

Bambach et al. [24] employed a polymer matrix carbon fiber-reinforced square section-reinforced composite in their study, and the damages that resulted from the experiment were investigated. Kakogiannis et al. [25] tested composite pipes after applying an axial dynamic impact force. The results proved that increasing the diameter of the composite material enhanced the maximum and total energy absorptions because of the trials. To forecast the mechanical and wear characteristics of short fiber-reinforced polyamide composites, Jiang et al. [26] used an ANN model. The neural networks were optimized after the polyamide composites were reinforced with short carbon and glass fibers. As a function of fiber composition and testing circumstances, a neural network was employed to predict mechanical and wear qualities. The best prediction of shear stress–strain behavior of carbon/epoxy and glass/epoxy fabric composites were analyzed by ANN in Ref. [27]. Khatir et al. [28–30] created an improved ANN based on different optimization techniques for damage identification in composite materials. Based on mechanical characterization and drilling tests, the implications of stacking sequence on the drilling machinability of filament wound hybrid composite pipes can be found in Ref. [31]. The impact identification of composite cylinders using a weighted fusion model and an enhanced deep metric learning model total least squares with Tikhonov regularization can be found in Ref. [32]. The results demonstrated that the suggested technique could achieve very low localization errors on three-dimensional composite structures and resilient and accurate reconstruction even the noise. This present study aims to develop a new model to predict the displacement of composite pipes after different impacts of low velocities using enhanced ANN. Jaya and E-Jaya are used to improve the ANN technique based on various parameters, such as input velocity, thickness, the number of layers, and stacking sequence. The obtained results show the advantage of E-Jaya compared with the Jaya algorithm to enhance the ANN technique. Recently, a novel application based on Physics-Informed Artificial Neural Network Architectures for System and Input Identification of Structural Dynamics was presented in Ref. [33]. The provided results showed the effectiveness of the presented application.

The structure of the present paper is divided into different sections. In Section 2, we describe the methodology of the improved ANN technique using Jaya and E-Jaya. Section 3 presents the experimental and numerical parameters required to build the data that can be used for the prediction. Results and discussion are reported in Section 4. Finally, the conclusion and remarks related to the proposed technique and its advantages to predict the displacement in the composite pipe using different low velocities are presented.

2. Improved ANN

Intelligent and nature-inspired solutions are now gaining a lot of attention in the real world when it comes to tackling complicated challenges. One of the most widely used and comprehensive intelligent systems is neural networks. Pattern recognition, identification, classification, image processing, and control systems are some of the sophisticated operations utilized by neural networks. This paper uses advanced optimization techniques to improve ANN for better prediction [8,34]. More details are discussed in the following sections.

2.1. Jaya and E-Jaya

As noted previously, Jaya performs its search process using a basic learning technique [35,36]. This strategy can be expressed as follows:

$$v_i = x_i + \lambda_1 \times (x_{Best} - |x_i|) - \lambda_2 \times (x_{Worst} - |x_i|), i = 1, 2, 3, \ldots, m \tag{1}$$

where λ_1 and λ_2 denote random numbers between [0–1]; m represents the population size; x_{Best} and x_{Worst} are the current best and the worst solution, respectively; and x_i and v_i are the solution and trail vectors of the ith individual, respectively. The second part of Equation (1) means the tendency of the solution x_i to move closer to the current best solution. Next, the last term represents the tendency of x_i to move away from the x_{Worst}. Furthermore, a better convergence speed can be presented in the next iteration, which can be shown in the following equation:

$$x_i \begin{cases} v_i \\ x_i \end{cases} \text{if } f(v_i) \leq f(x_i), \text{ otherwise} \tag{2}$$

where $f(*)$ denotes the objective function.

Population x_i in Jaya is initialized as follows:

$$x_i = l + (u - l) \times \lambda_3, i = 1, 2, 3, \ldots, N \tag{3}$$

where λ_3 presents a random number, and u and l denote the upper and lower limit variables, respectively.

Two strategies are used for E-Jaya. The first is based on a local exploitation strategy, and the second is based on a global exploration strategy. Lower and upper local attractors are considered to avoid the potential risk. The upper local attract point can be described as follows:

$$P_u = \lambda_3 \times x_{Best} + (1 - \lambda_3) \times M \tag{4}$$

where λ_3 denotes a random number in the interval [0–1], P_u denotes the upper local attract point, x_{Best} presents the current best solution, and M denotes the current mean solution.

Next, the following equation expresses the lower local attract point:

$$P_l = \lambda_4 \times x_{Worst} + (1 - \lambda_4) \times M \tag{5}$$

where x_{Worst} denotes the current worst solution, and λ_4 presents a random number in the interval [0–1].

Based on the last two equations, the local exploitation strategy of E-Jaya can be presented as:

$$v_i = x_i + \lambda_5 \times (P_u - x_i) - \lambda_6 \times (P_l - x_i), i = 1, 2, \ldots, N \tag{6}$$

where λ_5 and λ_6 denote a random number [0–1].

The second strategy is based on global exploration, and improving the global ability of the original algorithm, the main idea is based on the differential vectors between historical and contemporary populations having a greater solution space than differential vectors between populations of the same generation. The following equation expresses the presented strategy:

$$X_{old} \ (X_{old} = \{x_{old}, 1, x_{old}, 2, \ldots x_{old}, N\}) \tag{7}$$

First, it is generated by the following equation:

$$X_{old} \begin{cases} X \\ X_{old} \end{cases} \text{if } P_{Switch} \ \leq \ 0.5; \tag{8}$$

where X_{old} denotes the historical population, and P_{switch} denotes the switch probability.

The global exploration strategy of E-Jaya can be expressed by the following equation:

$$v_i = x_i + k \times (x_{old} - x_i), i = 1, 2, \ldots, N \tag{9}$$

where k denotes a random number.

2.2. Implementation of E-Jaya to Enhance ANN

An ANN can be used as a black-box model to connect complicated input and output datasets once it has been properly trained. More influential parameters in ANN weights and biases can help to connect the neurons together, as shown in Figure 1. w_{ij} presents the weights of neuron connection between the input node and neuron in the hidden layers. b_j denotes the bias associated with the jth neuron in the hidden layer.
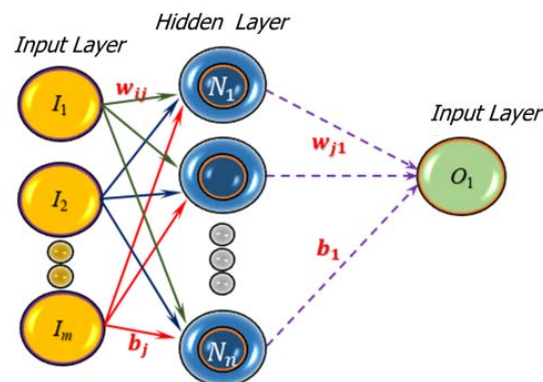

Figure 1. ANN architecture.

Additionally, w_j denotes the weight of neuron connection between the jth neuron in a hidden and single neuron in the output layers. Indices $i = 1, 2, \ldots, m$ represent the input features, and $j = 1, 2, \ldots, n$ represent hidden layer neurons. The total number of parameters used in the network is $n \times (m + 2) + 1$, and b_1 represents the bias associated with the single neuron in the output layer neuron. In this article, Jaya and E-Jaya are used to improve the parameters of ANN. The objective function is used to minimize the network root mean square error (RMSE). Four parameters are considered, namely input velocity, thickness, the number of layers, and stacking sequence to compute the displacement as output.

3. Experimental Validation

The data needed to train ANN models was generated by improved numerical simulations using the commercial FEA software Abaqus. The numerical model is required to be evaluated against previously proven numerical or experimental data, which is a standard procedure in numerical investigations. This section describes more details about numerical validation based on experimental analysis taken from Refs. [37,38].

3.1. Low-Velocity Impact Tests and Materials

The low-velocity impact responses of GFRP composite pipe samples were investigated using a specially developed low-velocity impact apparatus. In Figure 2, we can see the low-velocity impact instrument, specimen support, and anti-rebound system. V-shaped support with a 60° angle was used to fix the test specimens. We can obtain a single hit since the test stand contains an anti-rebound mechanism. A data logging system is also included in the test stand, which can send force signals at a sampling rate of 25 kHz.

Figure 2. (**a**) Low-velocity impact test stand and data logging system, (**b**) anti-rebound system, and (**c**) shore D hardness tester [37,38].

The anti-rebound system is engaged by dropping mass through a proximity sensor, which sends a signal to the PLC unit, where pneumatic pistons are actuated with a predetermined delay to prevent subsequent impacts. After the first impact, the anti-rebound device kept the impact mass, preventing repeated impacts. The force sensor transmits force signals from the origin to the termination of the impact to the data recording system and Signal Express software. Newton's law of motion is used to calculate the variance of contact force displacement and energy time. The considered diameter is Ø54, and composite pipes with $(\pm 55°)_3$ configurations were fabricated. In order to test the effect of low-velocity impact damage, composite pipes with a Ø54 diameter according to ASTM D 7136 at different velocities using five repeated tests were used. More details about the production of GFRP composite pipes can be found in Refs. [37,38].

3.2. FE Model

For this investigation, the data were extracted from numerical simulations using the commercial FEA software Abaqus explicit after validation with experimental data from Refs. [37,38]. Table 1 shows the geometric dimensions of the composite pipe and impactor information related to the radius, mass, and velocity. The mechanical properties of fiber and matrix are presented in Table 2. The mechanical properties and strength of GFRP layers can be obtained using the equations in Appendices A and B respectively.

Table 1. Geometric dimensions of the composite pipe and the impactor.

Composite Pipe		Impactor	
Length	155 (mm)	Radius	12 (mm)
Interior diameter	54 (mm)	Mass	5.6 (kg)
Exterior diameter	58.8 (mm)	Velocity	1.5, 2, 2.5 and 3 (m/s)

Table 2. Mechanical properties of fiber and matrix.

	E (GPa)	$\sigma_{tensile}$ (MPa)	ρ (g/cm^3)	$\varepsilon_{failure}$ (%)
Fiber: E-glass	73	2400	2.6	1.5–2
Matrix: Epoxy resin	3.4	50–60	1.2	4–6

Figure 3a shows the meshing of the composite pipe and the shape of the impactor, and Figure 3b shows the ply configuration. The material considered in this analysis is GFRP tubes. The geometry of the composite pipe is 3-D, which is meshed using the S4R shell elements (a four-node doubly curved thin or thick shell with reduced integration, hourglass control, and finite membrane strains). The friction coefficient [39,40] between all system parts (composite pipe/support–impactor/composite pipe) equals 0.3 in the present study. The load is applied in the form of initial velocity to the impactor, which equals the value of energy at the time of impact. The boundary conditions are considered by fixing the test specimens and simulating V-shaped support with a 60° angle.
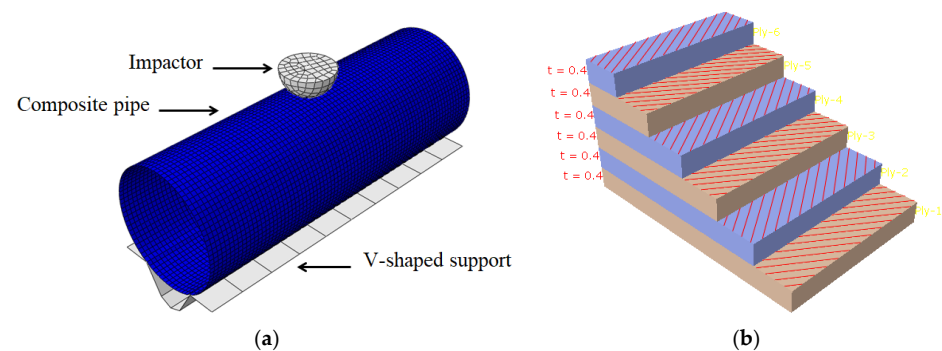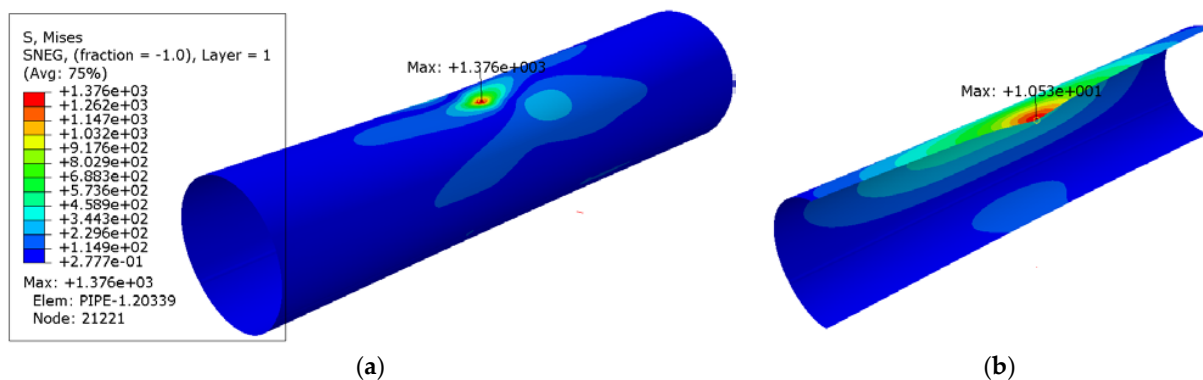

(**a**)　　　　　　　　　　　　　(**b**)

Figure 3. (**a**) FE model showing the composite pipe mesh, the impactor, and V-shaped support as a rigid solid, and (**b**) layup plot and material orientation (±55°).

Figure 4a,b shows the stress contour at the time of maximum contact and the displacement, where the impactor kinetic energy became zero.

(**a**)　　　　　　　　　　　　　(**b**)

Figure 4. (**a**) Stress contour at the instant of 6 ms coincident with zero kinetic energy of impactor and (**b**) max displacement during impact.

The obtained results based on experimental analysis are compared with developed FEA. The failure initiation was identified, and the damage was simulated using 3D Hashin failure criteria [41–43]. This criterion was applied in many studies and offered a more effective result in the damage evaluation in composite constructions. In the current study, this criterion is applied in all steps of the composite pipe's progressive damage. A suitable grid size is chosen, and the numerical solution's convergence with the elastic phase is confirmed. Using the S4R mesh type, we reduce the element size from 5 mm to 1 mm, as shown in Figure 5a,b:
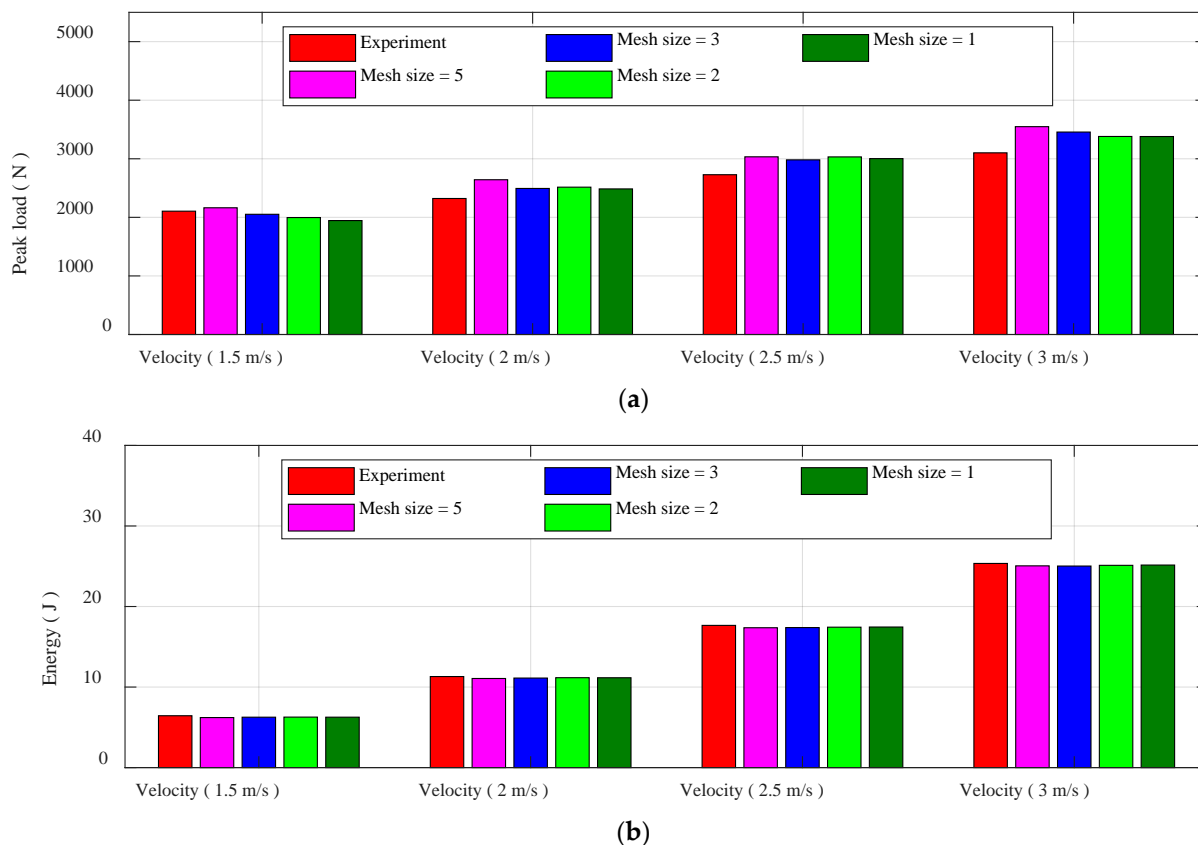

(**a**)

(**b**)

Figure 5. Different numerical outputs for different impact velocities and mesh size: (**a**) Peak load (N) and (**b**) energy (J).

The convergence study in terms of energy and the peak load during contact is shown in Figure 5a,b, where it is observed that the results of 1 mm and 2 mm element sizes are identical. The numerical results are then compared with experimental graph data following the convergence study. The force–time loading curves and energy–time curves have been generated by the 3D model. Figure 6 presents the peak load variation versus time under increasing impact velocities, and Figure 7 shows the variation of energy versus time for different velocities for a composite pipe with a diameter equal to Ø54 mm.
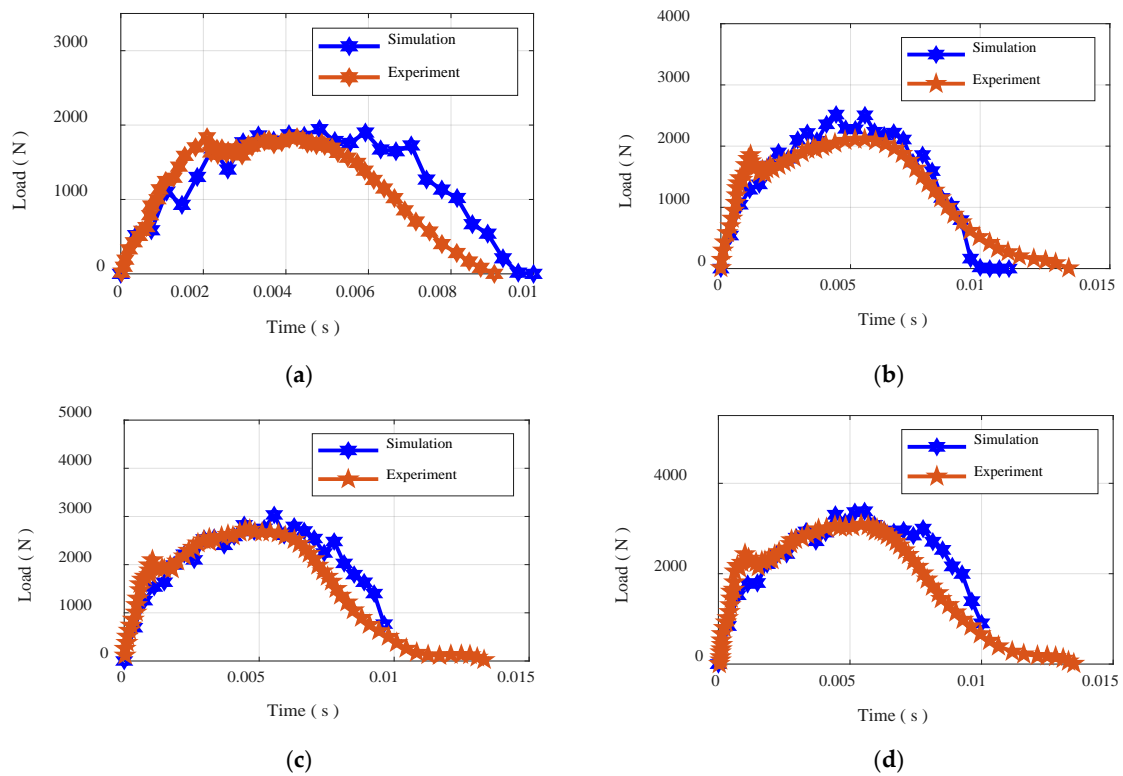
Figure 6. The peak load variation versus time under increasing impact velocities: (**a**) 1.5 m/s, (**b**) 2 m/s, (**c**) 2.5 m/s, and (**d**) 3 m/s.
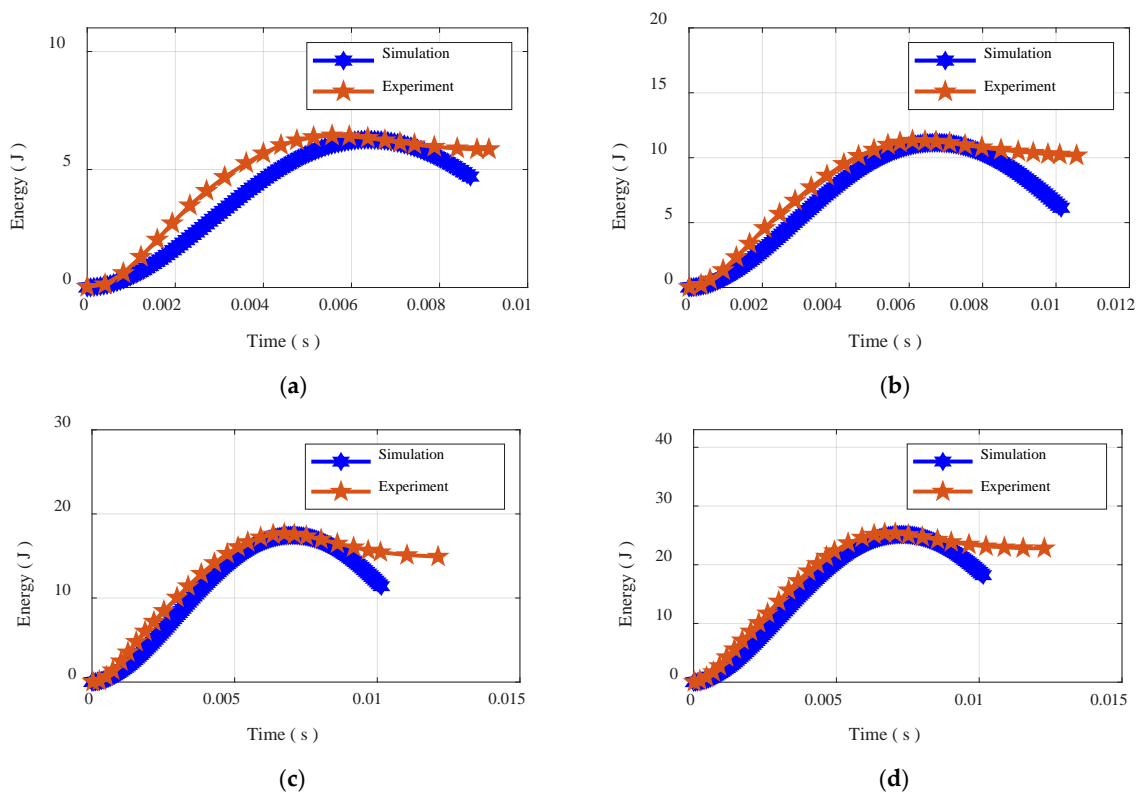

Figure 7. The energy variation versus time under increasing impact velocities: (**a**) 1.5 m/s, (**b**) 2 m/s, (**c**) 2.5 m/s, and (**d**) 3 m/s.

Based on the obtained results for different outputs (load-time data, energy-time data), the developed numerical model shows accurate results and acceptable error compared with the experimental results. This model is used in the next section to construct the data for several input cases.

3.3. Design of Experiments

The design of experiments is helpful during the data gathering phase because it offers a systematic and exact approach that produces reliable, tenable, and supportable datasets. The sensitivity analysis identifies different variables—impact velocity, composite pipe thickness, number of layers, and stacking sequence of material type—as being of particular importance when taking the impact behavior into account. As a result, the study here considers these four variables, and the various levels examined are provided in Table 3. The objective is to collect data on the peak displacement of the impactor for each pipe, from total pipe failure to just slight or minimal pipe damage.

Table 3. The obtained collected data from a developed numerical model used for training ANN-Jaya and ANN-E-Jaya.

Inputs								Outputs	
Velocity (m/s)		Thickness (mm)		Number of Layers		Stacking Sequence		Displacement (mm)	
Factors	Levels	Factors	Levels	Factors	Levels	Factors	Levels		
		1.3	1	4	1	($\pm$55)	1		
1.5	1	1.95	2	6	2				
2	2	2.6	3	8	3	($\pm$45)	2	-	
2.5	3	3.25	4	10	4				
3	4	3.9	5	12	5	($\pm$35)	3		
Min	Max	Min	Max	Min	Max			Min	Max
1.5	3	1.3	3.9	4	12	-		0.791289	19.906

A total of 75 numerical tests were run with various combinations of the earlier mentioned variables. The estimations were based on the maximum displacement at impact velocities of 1.5, 2, 2.5, and 3 m/s. In every investigation instance, the impactor's size and weight are kept constant. All the tests follow the same boundary conditions as well. The models were run in the Explicit setting of Abaqus software.

4. Results and Discussion

The present study highlights the utilization of a recently developed optimization technique, namely, E-Jaya, to effectively adapt the influenced parameters of artificial neural networks (ANN) during the training process. This study aims to compute the displacement of a composite pipe after low-velocity impacts, and thereby aid in selecting the best design before use. To investigate the efficacy of E-Jaya, it was tested alongside the original algorithm. Both optimization algorithms were subjected to a population size of 1000 and 500 iterations, while the best training was identified through the consideration of different hidden layer sizes (H) (i.e., 6, 8, 10, and 12). The training process for both optimization algorithms is presented in Figure 8.
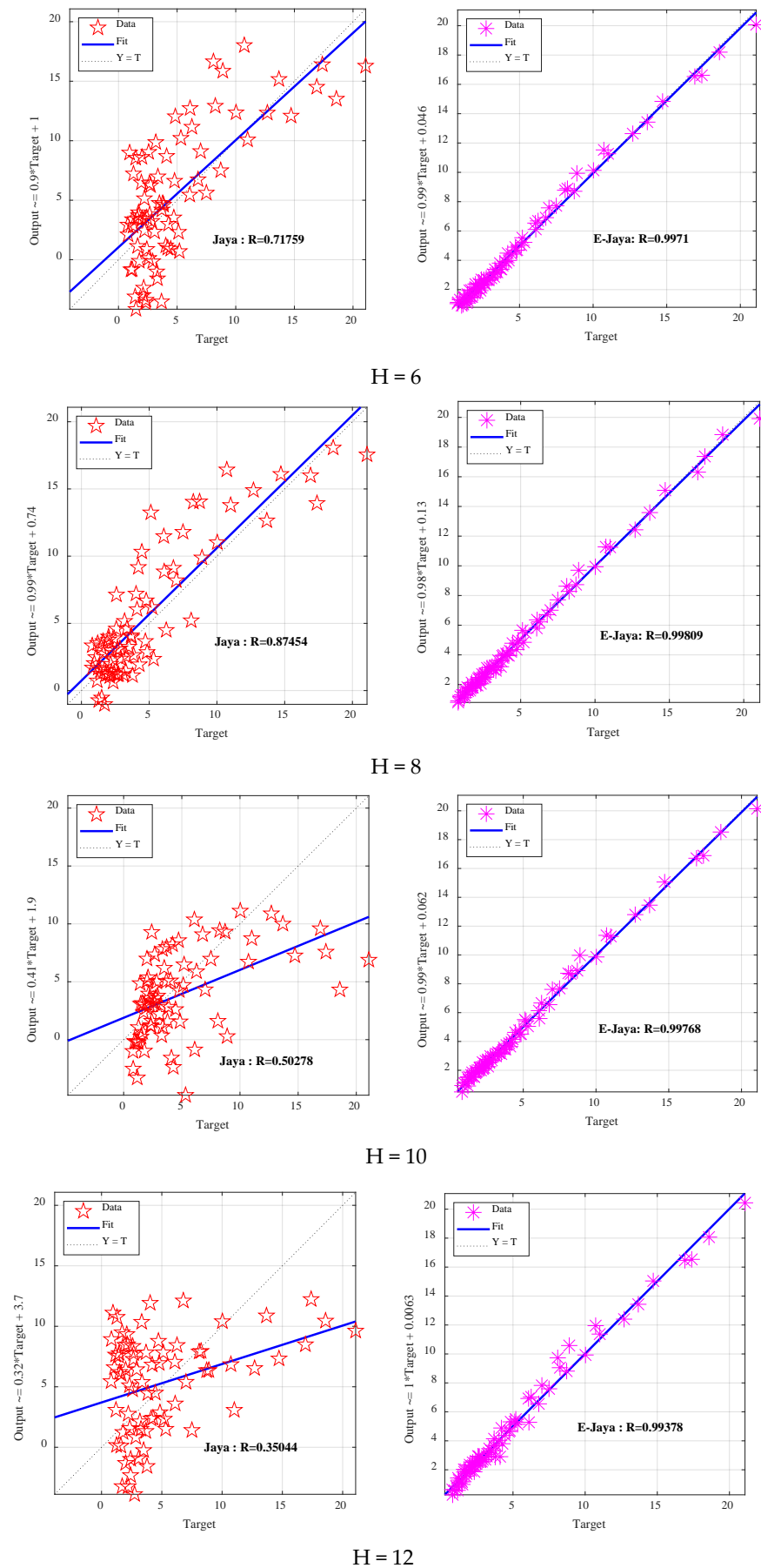
Figure 8. Regression analysis using Jaya and E-Jaya.

The effectiveness of the E-Jaya algorithm was compared with that of the Jaya algorithm for achieving better training to improve an artificial neural network (ANN) model. To achieve this analysis, 75 datasets from the developed numerical model were collected into the ANN model. The obtained results from this study demonstrate that better training can be achieved by using the E-Jaya algorithm with different hidden layer sizes compared with the Jaya algorithm. The successful adaptation of influenced parameters of ANN during the training process using E-Jaya led to improved accuracy in computing the displacement of a composite pipe after low-velocity impacts. This indicates the effectiveness of E-Jaya as an optimization technique for enhancing the performance of ANN in material testing and design.

To further demonstrate the effectiveness of the E-Jaya algorithm, six scenarios were tested, considering CPU time, with varying hidden layer sizes. The presented results of these tests are summarized in Table 4a–d. These results highlight the benefits of using the E-Jaya algorithm for achieving better training and improving accuracy in material testing and design.

In the present study, the performance of the E-Jaya algorithm was evaluated in comparison with the Jaya algorithm based on the accuracy of the obtained results. The CPU time for both algorithms was also compared across different cases.

The results demonstrate that the E-Jaya algorithm outperforms the Jaya algorithm in terms of accuracy for all cases. Additionally, the CPU time is lower when using the E-Jaya algorithm as compared with the Jaya algorithm. These findings indicate that the E-Jaya algorithm has the potential to provide faster predictions as compared with the finite element method (FEM).

The discrepancies between the actual results, as well as, the results obtained from the E-Jaya and Jaya algorithms, were further summarized. This analysis provides a detailed overview of the effectiveness of both algorithms in achieving accurate predictions for the given application in Figure 9a–d.

The present study aimed to evaluate the performance of an enhanced artificial neural network (ANN) model using E-Jaya with different hidden layer sizes for composite pipes. The correlation data obtained from this study showed that the enhanced ANN using E-Jaya with eight neurons outperformed the other networks for composite pipes.

The correlation coefficient, denoted as R, was used to evaluate the level of accuracy of the ANN model. The enhanced ANN model using E-Jaya with eight hidden layer sizes achieves a high level of accuracy, with an R value of 0.998. This is significantly higher than the other hidden layer sizes and the original algorithm.

The results of this study underscore the potential of the E-Jaya algorithm in enhancing the performance of ANN for composite pipes. The use of E-Jaya with eight hidden layer sizes resulted in a highly accurate ANN model for composite pipes, which can support the design and testing of these materials.

Further research on the utilization of E-Jaya in other applications is warranted to determine its broader applicability and efficacy. Moreover, investigating the impact of varying parameters, such as the number of iterations and the population size, on the performance of the ANN model can further enhance its accuracy and applicability.
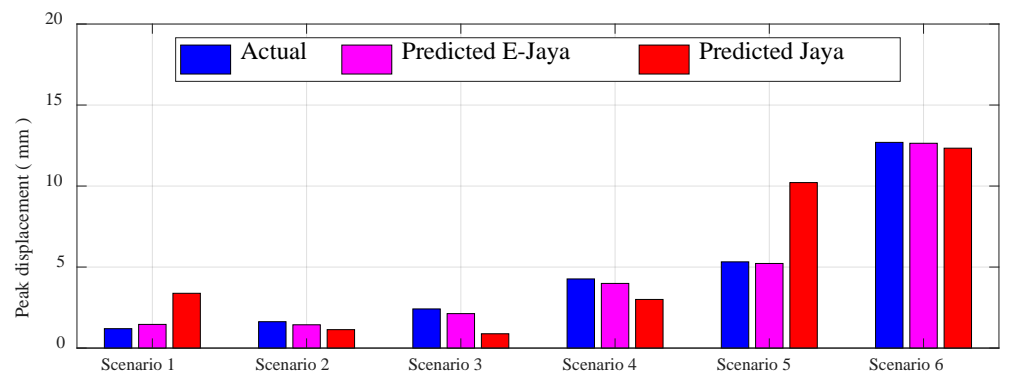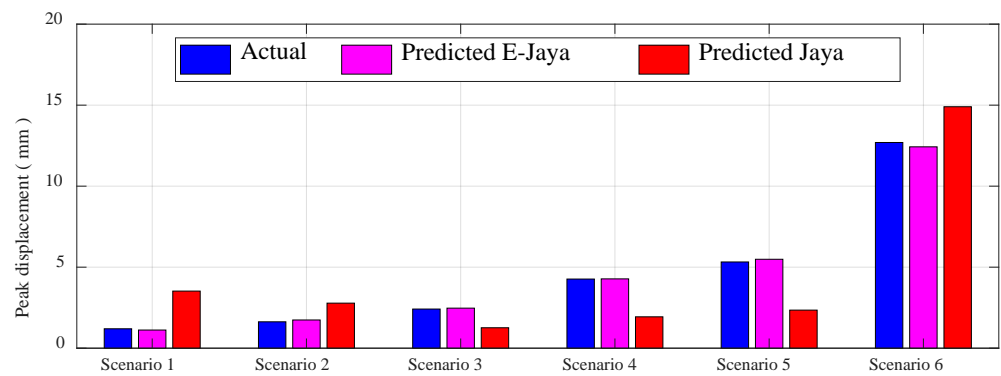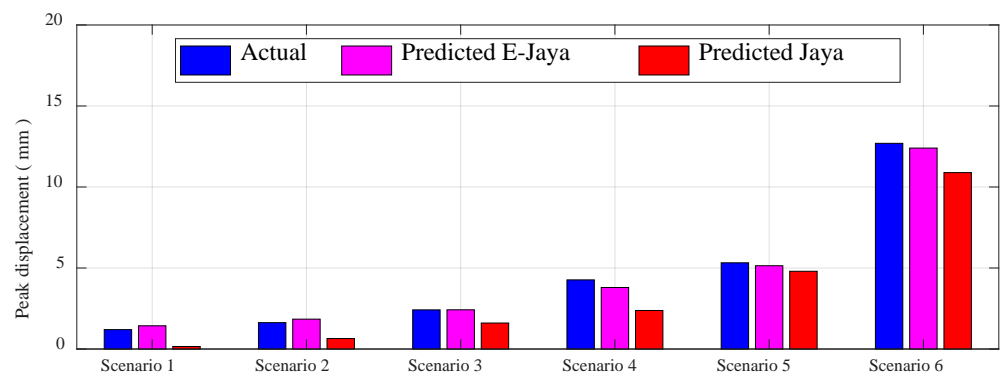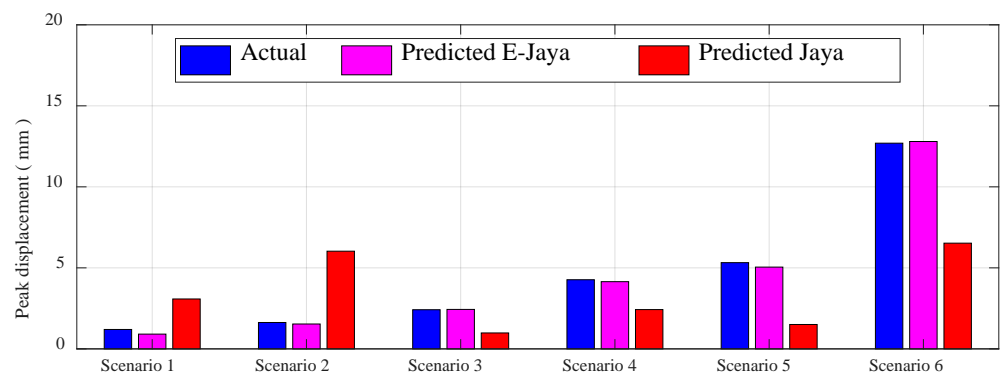
Figure 9. Peak displacement prediction for six scenarios: (**a**) H = 6, (**b**) H = 8, (**c**) H = 10, (**d**) H = 12.

Table 4. Independent scenarios to verify Jaya and E-Jaya model: (a) H = 6, (b) H = 8, (c) = 10 and (d) = 12.

Hidden = 6				Actual peak displacement	Simulated peak displacement	Difference (Absolute value)	Simulated peak displacement	Difference	CPU (Jaya)	CPU (E-Jaya)
V	T	N	S	(Abaqus) mm	(Jaya) mm		(E-Jaya) mm			
1.5	4.8	12	3	1.1977	3.3815	2.1838	1.4611	0.2634		
1.5	4	10	3	1.6282	1.1378	0.4904	1.4375	0.1907		
2	4	10	2	2.4162	0.8834	1.5328	2.1267	0.2895	3746.557	3070.96
2.5	3.2	8	2	4.2674	3.0015	1.2659	3.9907	0.2767		
3	3.2	8	2	5.3216	10.2138	4.8922	5.2222	0.0994		
2	1.6	4	1	12.6957	12.3378	0.3579	12.6404	0.0553		

(a) H = 6

Hidden = 8				Actual peak displacement	Simulated peak displacement	Difference	Simulated peak displacement	Difference	CPU (Jaya)	CPU (E-Jaya)
V	T	N	S	(Abaqus) mm	(Jaya) mm		(E-Jaya) mm			
1.5	4.8	12	3	1.1977	3.5246	2.3269	1.1204	0.0773		
1.5	4	10	3	1.6282	2.7805	1.1523	1.7411	0.113		
2	4	10	2	2.4162	1.2612	1.155	2.4716	0.0555	3711.569	3113.85
2.5	3.2	8	2	4.2674	1.936	2.3314	4.278	0.0106		
3	3.2	8	2	5.3216	2.35	2.9716	5.4882	0.1666		
2	1.6	4	1	12.6957	14.9022	2.2065	12.4277	0.268		

(b) H = 8

Hidden = 10				Actual peak displacement	Simulated peak displacement	Difference	Simulated peak displacement	Difference	CPU (Jaya)	CPU (E-Jaya)
V	T	N	S	(Abaqus) mm	(Jaya) mm		(E-Jaya) mm			
1.5	4.8	12	3	1.1977	0.1565	1.3542	1.4344	0.2367		
1.5	4	10	3	1.6282	0.6487	0.9795	1.8452	0.217		
2	4	10	2	2.4162	1.6043	0.8119	2.4206	0.0044	3718.516	3068.287
2.5	3.2	8	2	4.2674	2.379	6.6464	3.7983	0.4691		
3	3.2	8	2	5.3216	4.7983	10.1199	5.1405	0.1811		
2	1.6	4	1	12.6957	10.8877	1.808	12.4026	0.2931		

(c) H = 10

Hidden = 12				Actual peak displacement	Simulated peak displacement	Difference	Simulated peak displacement	Difference	CPU (Jaya)	CPU (E-Jaya)
V	T	N	S	(Abaqus) mm	(Jaya) mm		(E-Jaya) mm			
1.5	4.8	12	3	1.1977	3.0797	1.882	0.9108	0.2869		
1.5	4	10	3	1.6282	6.0291	4.4009	1.5353	0.0929		
2	4	10	2	2.4162	0.9828	3.399	2.4353	0.0191	3741.412	3093.343
2.5	3.2	8	2	4.2674	2.4248	1.8426	4.1478	0.1196		
3	3.2	8	2	5.3216	1.5051	3.8165	5.0469	0.2747		
2	1.6	4	1	12.6957	6.5249	6.1708	12.7985	0.1028		

(d) H = 12

Notation: V: Velocity (m/s); T: Thickness (mm); N: Number of layers; S: Stacking sequence.

5. Conclusions

In this study, the effectiveness and robustness of the algorithms to improve the training of ANN and its ability to predict displacement are discussed. Two parameters, bias and weight, including different hidden layer sizes (6, 8, 10, and 12), are considered to enhance the ANN model. The data used for this study were extracted from the numerical model using FEM after validation with experimental tests. The study presents an enhanced ANN algorithm, based on the E-Jaya algorithm, for predicting the displacement in composite pipes subjected to low-velocity impact loads. The study investigates the damages induced by impact velocities of 1.5, 2, 2.5, and 3 m/s on composite pipes with a diameter of 54 mm. The results demonstrate that the E-Jaya algorithm is effective in training and predicting displacement, outperforming the original algorithm. This study highlights the

importance of predicting low-velocity impact behavior in composite pipes, which can lead to internal damage and stiffness loss. The findings of this study can support the design of composite pipes with improved impact resistance and reduce the risk of internal damage and pressure leakage. The study contributes to the existing knowledge on the behavior of fiber-reinforced polymers under impact loads and provides a new methodology for enhancing ANN algorithms for better prediction accuracy. Future research can explore the effectiveness of other ANN algorithms in predicting the impact response of composite pipes under different loading conditions. This study has significant implications for the design and application of composite pipes in various industries, including civil and mechanical engineering structures.

Author Contributions: Conceptualization, S.K.; Methodology, S.K., M.A.W. and B.B.; Software, S.K. and B.B.; Validation, S.K. and M.A.W.; Formal analysis, S.K., E.G., E.M.B. and A.M.A.; Investigation, S.K., E.G., M.A.W., E.M.B., B.B. and A.M.A.; Data curation, S.K.; Writing—review & editing, S.K., E.G., B.B. and M.A.W.; Visualization, E.M.B.; Funding acquisition, A.M.A. and E.G. All authors have read and agreed to the published version of the manuscript.

Data Availability Statement: The Matlab code of the enhanced Jaya-ANN can be found at https://github.com/Samir-Khatir/Enhanced-ANN-Real-application-in-composite-pipe.

Conflicts of Interest: The authors declare no conflict of interest.

Appendix A

Micromechanics rules for mechanical properties of GFRP layers [44–46]. Mechanical properties of the GFRP layers can be obtained using the equations below:

$$E_x = E_f V_f + E_m V_m \tag{A1}$$

$$\nu_{xy} = \nu_f V_f + \nu_m V_m \tag{A2}$$

$$E_y = \frac{E_f E_m (E_m + E_f V_f - E_m V_f)}{E_f{}^2(-2 + V_f)(-1 + V_f)V_f{}^2 + E_m{}^2(-1 + V_f)^2(1 + V_f)V_f + E_f E_m(1 + 2V_f(-1 + V_f)(1 + (-1 + V_f)V_f))} \tag{A3}$$

$$G_{xy} = \frac{G_m}{1 - \sqrt{V_f}(1 - \frac{G_m}{G_f})} \tag{A4}$$

$$E_{zz} = E_y; \quad G_{xz} = G_{xy}; \quad G_{yz} = E_y/(2 + 2\nu_{yz}); \quad \nu_{xz} = \nu_{yz} = 0.2 \tag{A5}$$

$$\rho_{GFRP} = (V_f \rho_f + V_m \rho_m) \tag{A6}$$

Appendix B

Calculating the strength of GFRP layers [44]:

$$X_T = X_f(V_f + V_m \frac{E_m}{E_f}) \tag{A7}$$

$$X_C = 0.5X_T \tag{A8}$$

$$Y_T = V_m X_m \tag{A9}$$

$$Y_C = V_m X_m{'} \tag{A10}$$

where X_T, X_C, Y_T, and Y_C denote the longitudinal tensile strength, longitudinal compressive strength, transverse tensile strength, and transverse compressive strength of GFRP plies. X_f, X_m, and $X_m{'}$ stand for fiber tensile strength, matrix tensile strength, and matrix compressive strength, respectively.

References

1. Davies, G.A.O.; Olsson, R. Impact on composite structures. *Aeronaut. J.* **2016**, *108*, 541–563. [CrossRef]
2. Chib, A. Parametric Study of Low Velocity Impact Analysis on Composite Tubes. Ph.D. Thesis, Wichita State University, Wichita, KS, USA, 2006.
3. Kersys, A.; Kersiene, N.; Ziliukas, A. Experimental Research of the Impact Response of E-Glass/Epoxy and Carbon/Epoxy Composite Systems. *Mater. Sci.* **2010**, *16*, 4.
4. Karakuzu, R.; Erbil, E.; Aktas, M. Impact characterization of glass/epoxy composite plates: An experimental and numerical study. *Compos. Part B Eng.* **2010**, *41*, 388–395. [CrossRef]
5. Li, C.F.; Hu, N.; Yin, Y.J.; Sekine, H.; Fukunaga, H. Low-velocity impact-induced damage of continuous fiber-reinforced composite laminates. Part I. An FEM numerical model. *Compos. Part A Appl. Sci. Manuf.* **2002**, *33*, 1055–1062. [CrossRef]
6. Tita, V.; de Carvalho, J.; Vandepitte, D. Failure analysis of low velocity impact on thin composite laminates: Experimental and numerical approaches. *Compos. Struct.* **2008**, *83*, 413–428. [CrossRef]
7. Benaissa, B.; Hocine, N.A.; Khatir, S.; Riahi, M.K.; Mirjalili, S. YUKI algorithm and POD-RBF for Elastostatic and dynamic crack identification. *J. Comput. Sci.* **2021**, *55*, 101451. [CrossRef]
8. Shirazi, M.I.; Khatir, S.; Benaissa, B.; Mirjalili, S.; Wahab, M.A. Damage assessment in laminated composite plates using Modal Strain Energy and YUKI-ANN algorithm. *Compos. Struct.* **2022**, *303*, 116272. [CrossRef]
9. Benaissa, B.; Khatir, S.; Jouini, M.S.; Riahi, M.K. Optimal Axial-Probe Design for Foucault-Current Tomography: A Global Optimization Approach Based on Linear Sampling Method. *Energies* **2023**, *16*, 2448. [CrossRef]
10. Iannucci, L.; Willows, M.L. An energy based damage mechanics approach to modelling impact onto woven composite materials— Part I: Numerical models. *Compos. Part A Appl. Sci. Manuf.* **2006**, *37*, 2041–2056. [CrossRef]
11. Khatir, S.; Tiachacht, S.; Benaissa, B.; Le Thanh, C.; Capozucca, R.; Abdel Wahab, M. Damage Identification in Frame Structure Based on Inverse Analysis. In Proceedings of the 2nd International Conference on Structural Damage Modelling and Assessment, Ghent, Belgium, 4–5 August 2021; pp. 197–211.
12. Kahouadji, A.; Tiachacht, S.; Slimani, M.; Behtani, A.; Khatir, S.; Benaissa, B. Vibration-Based Damage Assessment in Truss Structures Using Local Frequency Change Ratio Indicator Combined with Metaheuristic Optimization Algorithms. In Proceedings of the International Conference of Steel and Composite for Engineering Structures, Ancona, Italy, 12–13 September 2022; pp. 171–185.
13. Slimani, M.; Khatir, T.; Tiachacht, S.; Boutchicha, D.; Benaissa, B. Experimental sensitivity analysis of sensor placement based on virtual springs and damage quantification in CFRP composite. *J. Mater. Eng. Struct.* **2022**, *9*, 207–220.
14. Slimani, M.; Tiachacht, S.; Behtani, A.; Khatir, T.; Khatir, S.; Benaissa, B.; Riahi, M.K. Improved ANN for Damage Identification in Laminated Composite Plate. In Proceedings of the International Conference of Steel and Composite for Engineering Structures, Ancona, Italy, 12–13 September 2022; pp. 186–198.
15. Doyum, A.B.; Altay, B. Low-velocity impact damage in glass fibre/epoxy cylindrical tubes. *Mater. Des.* **1997**, *18*, 131–135. [CrossRef]
16. Rafiee, R.; Ghorbanhosseini, A.; Rezaee, S. Theoretical and numerical analyses of composite cylinders subjected to the low velocity impact. *Compos. Struct.* **2019**, *226*, 111230. [CrossRef]
17. Çitil, Ş.; Ayaz, Y.; Temiz, Ş.; Aydın, M.D. Mechanical behaviour of adhesively repaired pipes subject to internal pressure. *Int. J. Adhes. Adhes.* **2017**, *75*, 88–95. [CrossRef]
18. Meijer, G.; Ellyin, F. A failure envelope for $\pm 60°$ filament wound glass fibre reinforced epoxy tubulars. *Compos. Part A Appl. Sci. Manuf.* **2008**, *39*, 555–564. [CrossRef]
19. Kara, M.; Uyaner, M.; Avci, A.; Akdemir, A. Effect of non-penetrating impact damages of pre-stressed GRP tubes at low velocities on the burst strength. *Compos. Part B Eng.* **2014**, *60*, 507–514. [CrossRef]
20. Kara, M.; Kırıcı, M. Effects of the number of fatigue cycles on the impact behavior of glass fiber/epoxy composite tubes. *Compos. Part B Eng.* **2017**, *123*, 55–63. [CrossRef]
21. Gning, P.B.; Tarfaoui, M.; Collombet, F.; Riou, L.; Davies, P. Damage development in thick composite tubes under impact loading and influence on implosion pressure: Experimental observations. *Compos. Part B Eng.* **2005**, *36*, 306–318. [CrossRef]
22. Malik, M.H.; Arif, A.F.M. ANN prediction model for composite plates against low velocity impact loads using finite element analysis. *Compos. Struct.* **2013**, *101*, 290–300. [CrossRef]
23. Maziz, A.; Tarfaoui, M.; Gemi, L.; Rechak, S.; Nachtane, M. A progressive damage model for pressurized filament-wound hybrid composite pipe under low-velocity impact. *Compos. Struct.* **2021**, *276*, 114520. [CrossRef]

24. Bambach, M.R.; Elchalakani, M.; Zhao, X.L. Composite steel–CFRP SHS tubes under axial impact. *Compos. Struct.* **2009**, *87*, 282–292. [CrossRef]
25. Kakogiannis, D.; Chung Kim Yuen, S.; Palanivelu, S.; Van Hemelrijck, D.; Van Paepegem, W.; Wastiels, J.; Vantomme, J.; Nurick, G.N. Response of pultruded composite tubes subjected to dynamic and impulsive axial loading. *Compos. Part B Eng.* **2013**, *55*, 537–547. [CrossRef]
26. Jiang, Z.; Gyurova, L.; Zhang, Z.; Friedrich, K.; Schlarb, A.K. Neural network based prediction on mechanical and wear properties of short fibers reinforced polyamide composites. *Mater. Des.* **2008**, *29*, 628–637. [CrossRef]
27. Bezerra, E.M.; Ancelotti, A.C.; Pardini, L.C.; Rocco, J.A.F.F.; Iha, K.; Ribeiro, C.H.C. Artificial neural networks applied to epoxy composites reinforced with carbon and E-glass fibers: Analysis of the shear mechanical properties. *Mater. Sci. Eng. A* **2007**, *464*, 177–185. [CrossRef]
28. Khatir, S.; Tiachacht, S.; Le Thanh, C.; Ghandourah, E.; Mirjalili, S.; Abdel Wahab, M. An improved Artificial Neural Network using Arithmetic Optimization Algorithm for damage assessment in FGM composite plates. *Compos. Struct.* **2021**, *273*, 114287. [CrossRef]
29. Zenzen, R.; Khatir, S.; Belaidi, I.; Le Thanh, C.; Abdel Wahab, M. A modified transmissibility indicator and Artificial Neural Network for damage identification and quantification in laminated composite structures. *Compos. Struct.* **2020**, *248*, 112497. [CrossRef]
30. Khatir, A.; Capozucca, R.; Khatir, S.; Magagnini, E.; Benaissa, B.; Le Thanh, C.; Wahab, M.A. A new hybrid PSO-YUKI for double crack identification in CFRP cantilever beam. *Compos. Struct.* **2023**, *311*, 116803. [CrossRef]
31. Gemi, L.; Köklü, U.; Yazman, Ş.; Morkavuk, S. The effects of stacking sequence on drilling machinability of filament wound hybrid composite pipes: Part-1 mechanical characterization and drilling tests. *Compos. Part B Eng.* **2020**, *186*, 107787. [CrossRef]
32. Li, S.; Peng, G.; Ji, M.; Cheng, F.; Chen, Z.; Li, Z. Impact identification of composite cylinder based on improved deep metric learning model and weighted fusion Tikhonov regularized total least squares. *Compos. Struct.* **2022**, *283*, 115144. [CrossRef]
33. Moradi, S.; Duran, B.; Eftekhar Azam, S.; Mofid, M. Novel Physics-Informed Artificial Neural Network Architectures for System and Input Identification of Structural Dynamics PDEs. *Buildings* **2023**, *13*, 650. [CrossRef]
34. Amoura, N.; Benaissa, B.; Al Ali, M.; Khatir, S. Deep Neural Network and YUKI Algorithm for Inner Damage Characterization Based on Elastic Boundary Displacement. In Proceedings of the International Conference of Steel and Composite for Engineering Structures, Ancona, Italy, 12–13 September 2022; pp. 220–233.
35. Rao, R. Jaya: A simple and new optimization algorithm for solving constrained and unconstrained optimization problems. *Int. J. Ind. Eng. Comput.* **2016**, *7*, 19–34.
36. Syafruddin, W.A.; Köppen, M.; Benaissa, B. Does the Jaya Algorithm Really Need No Parameters? In Proceedings of the 10th International Joint Conference on Computational Intelligence (IJCCI 2018), Seville, Spain, 18–20 September 2018; pp. 264–268.
37. Gemi, D.S.; Şahin, Ö.S.; Gemi, L. Experimental investigation of the effect of diameter upon low velocity impact response of glass fiber reinforced composite pipes. *Compos. Struct.* **2021**, *275*, 114428. [CrossRef]
38. Gemi, L.; Kayrıcı, M.; Uludağ, M.; Gemi, D.S.; Şahin, Ö.S. Experimental and statistical analysis of low velocity impact response of filament wound composite pipes. *Compos. Part B Eng.* **2018**, *149*, 38–48. [CrossRef]
39. Lancaster, J.K. The effect of carbon fibre reinforcement on the friction and wear of polymers. *J. Phys. D Appl. Phys.* **1968**, *1*, 549. [CrossRef]
40. Schön, J. Coefficient of friction of composite delamination surfaces. *Wear* **2000**, *237*, 77–89. [CrossRef]
41. Xin, S.H.; Wen, H.M. A progressive damage model for fiber reinforced plastic composites subjected to impact loading. *Int. J. Impact Eng.* **2015**, *75*, 40–52. [CrossRef]
42. Bsisu, K.A.-D.; Hussein, H.H.; Sargand, S.M. The Use of Hashin Damage Criteria, CFRP–Concrete Interface and Concrete Damage Plasticity Models in 3D Finite Element Modeling of Retrofitted Reinforced Concrete Beams with CFRP Sheets. *Arab. J. Sci. Eng.* **2017**, *42*, 1171–1184. [CrossRef]
43. Duarte, A.P.C.; Díaz Sáez, A.; Silvestre, N. Comparative study between XFEM and Hashin damage criterion applied to failure of composites. *Thin-Walled Struct.* **2017**, *115*, 277–288. [CrossRef]
44. Rafiee, R.; Reshadi, F. Simulation of functional failure in GRP mortar pipes. *Compos. Struct.* **2014**, *113*, 155–163. [CrossRef]
45. Masoumi, M.; Abdellahi, S.B.; Hejazi, S.M. Investigation flexural behavior of hybrid-reinforced layered filament wound pipes using experimental tests and numerical model. *J. Ind. Text.* **2022**, *51*, 5219S–5242S. [CrossRef]
46. Gay, D. *Composite Materials: Design and Applications*; CRC Press: Boca Raton, FL, USA, 2022.